Progress In Electromagnetics Research C, Vol. 8, 43–55, 2009

THE STUDY OF STRUCTURE-DEPENDENT PROPERTIES OF THIN MAGNETIC FILMS AT MICROWAVES BY FIELD-DOMAIN RESONANCE TECHNIQUE

S. N. Starostenko and K. N. Rozanov

Institute for Theoretical and Applied Electromagnetics
Russian Academy of Sciences
Russia

Abstract—The strip-line frequency-domain technique for permeability measurement is compared to the field domain technique. The combined setup for microwave measurement of thin film permeability with both techniques is proposed. The field-domain technique is less affected by inhomogeneity of measurement strip cell and has significantly higher signal-to-noise ratio, but the obtained parameters are affected by film thickness and may differ from that of the frequency-domain technique. Analysis of the field-domain data obtained at a set of frequencies makes it possible to determine the saturation magnetisation, the anisotropy field and the damping factor without the knowledge of the amount of substance under study. In case of a simple permeability spectrum the data on metal thickness make it possible to estimate the effective skin-depth as well. The technique is tested by simulation and is applied to determine permeability of Fe-based films vacuum-sputtered on glassceramic and polymer substrates.

1. INTRODUCTION

For the characterisation of microwave permeability of metal films two measurement techniques are frequently used: the sweep-frequency measurements of permittivity/permeability spectra of laminated samples with the help of vector network analysers (SF-VNA technique) and the conventional ferromagnetic resonance fixed frequency/sweep bias measurements (SB-FMR technique) that are usually performed in a high-quality cavity [1–4]. The SF-VNA technique is popular as it is fast and simple and the obtained permittivity/permeability data

Corresponding author: S. N. Starostenko (ssn@itael.ru).

can be directly used in the engineering practice, but the samples under study are relatively large and unsaturated. The SB-FMR technique is much more sensitive [2, 3], the sample is uniformly magnetised but the calculated permeability data may differ from that ones obtained under zero bias and the technique is poorly suited for measurements within a range of frequencies. The SF-VNA measurements are performed under non-zero external bias as well [5, 6], but the sensitivity of SF-VNA technique is much lower than that of SB-FMR one even in case of the resonance enhancement [7] as the measurement errors (the signal to noise ratio, SNR) are defined by calibration accuracy of a measurement cell [4]. The SF-VNA measurements are usually performed either in a coaxial line or in a strip-line. The coaxial cell is readily calibrated by standard technique [8] and is much more uniform than the strip line. The problem is that the measured washer samples are usually wound of film stripes, therefore the coaxial measurements are limited to flexible substrates and the obtained data are distorted by magnetostriction [5, 6, 10, 11]. The stripe cells are calibrated less accurately and the measurements inherit the problems of radiation into surrounding space [4, 7].

We develop a combined technique that is based on equipment standard for SF-VNA measurements, but exploits the advantages of swept bias and deals with samples large enough for engineering applications such as mobile antennas, absorbers, etc. Contrary to the standard SB-FMR technique where the measured power reflectivity R_P is assumed to correspond to imaginary permeability μ'', the proposed procedure takes into account the electrical dimensions of the sample, as the reflectivity minima may not correspond to the peak of magnetic absorption $\mu''_{\max}$ because of the resonance on sample size. The minimal reflectivity for a shorted sample is observed at quarterwave electrical thickness that depends on permittivity ε as well [4]. The coaxial-to-strip junction inhomogeneity, the effects of non-uniform field inside the cell and the permittivity contribution are taken into account by measurement of a reference sample with known constitutive parameters. The calculation of complex permeability μ from the measured complex reflection coefficient R is identical to the published procedure [4, 7].

Another advantage of the proposed technique is the ability to separate the composition-dependent properties of a permeable film (the saturation magnetisation M_S) from the structure-dependent ones (the anisotropy field H_A and the damping factor).

The outline of the article is as follows: experimental technique, theoretical background and comparison of SB-FMR and SF-VNA measurements, contribution of eddy currents, simulation and

properties of magnetron-sputtered Fe-based films, conclusions.

2. EXPERIMENTAL TECHNIQUE

The experimental setup (Fig. 1) includes a strip cell connected to VNA HP8720. The swept bias applied parallel to the cell axis is provided by an electromagnet, the bias strength H_{bias} is measured with a Hall sensor. The resonant amplification at a set of frequencies is obtained if necessary for samples with low permeance factor (the product of magnetic susceptibility and sample cross-section) by connecting the cell to VNA through an impedance inhomogeneity with a coaxial cable section. The inhomogeneity value defines the amplification, while the cable length defines the number of resonance frequencies [6].

The cell design [6] is schematically shown in the insert in Fig. 1; its dimensions are: $a = 27\,\text{mm}$, $w = 8\,\text{mm}$, $h_{cell} = 1.5\,\text{mm}$, $d_{cell} = 350\,\text{mm}$. The samples under study are stripes of metal films magnetron-sputtered on a rigid or flexible substrates; the metal thickness varies from $\sim$0.3 to 2 μm. The reference samples used for cell calibration are stripes of synthetic rubber filled with carbonyl iron. The permittivity ε and permeability μ of a reference sample are determined by standard SF-VNA measurements in a shorted and opened coaxial line [8]. The typical size of the samples is as follows: the length is $\sim$30 mm, the width is $3 \div 10\,\text{mm}$, and the thickness d is $0.02 \div 0.5\,\text{mm}$.

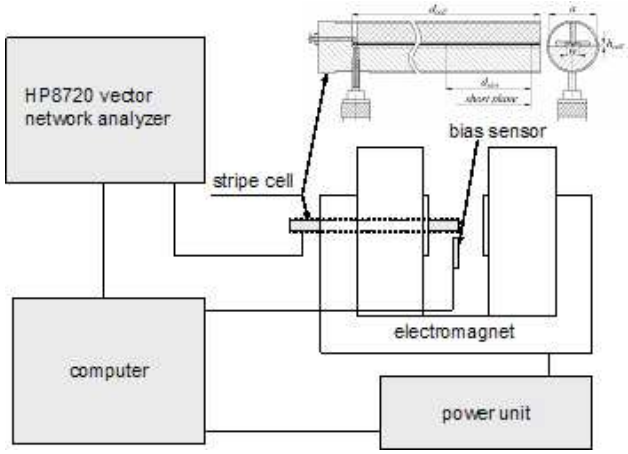

Figure 1. The diagram of an experimental setup and the design of a single-port strip cell.

The strip-line and the adjusted matched junction are functional up to 10 GHz but the dimensions (2×50 mm) of the slot for sample insertion restrict the SF-VNA range by $\sim$6 GHz because of the radiation from the cell.

3. THEORY OF SB-FMR AND SF-VNA TECHNIQUES

The treatment of permeability data is based on the Landau-Lifshitz-Gilbert (LLG) relation [3] simplified for the case of a thin film [10] with two demagnetising factors equal to zero:

$$\mu(f, H_{bias}) \approx 1 + \frac{\left(\frac{M_S}{f/\gamma\mu_{vac}}\right)^2}{\left(\frac{\sqrt{M_S(H_A+H_{bias})}}{f/\gamma\mu_{vac}}\right)^2 - 1 + i\alpha\sqrt{\frac{M_S}{H_A+H_{bias}}}\frac{\sqrt{M_S(H_A+H_{bias})}}{f/\gamma\mu_{vac}}} \quad (1)$$

where M_S is the saturation magnetisation of the film, H_A is the anisotropy filed, H_{bias} is the bias strength, f is the measurement frequency, $\gamma = 2.8$ GHz/kOe is the gyromagnetic factor, $\mu_{vac} = 1.257 \times 10^{-6}$ Hn/m and α is the Gilbert damping factor.

The relation (1) describes a permeability surface on the plane of frequency and bias strength. Fig. 2(a) shows the imaginary part

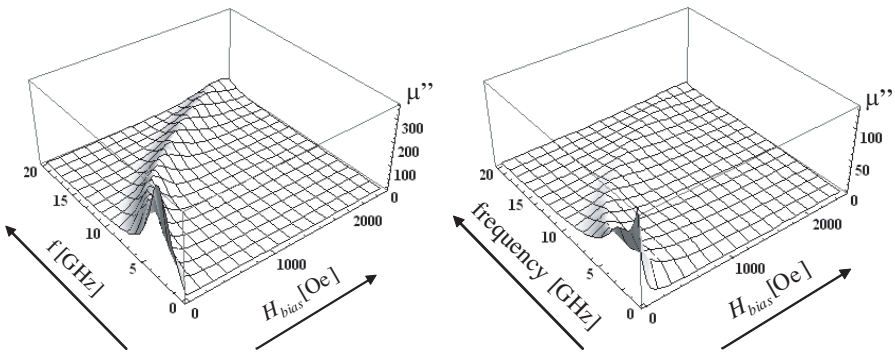

(a) (b)

Figure 2. (a) The surface of imaginary part of permeability described by relation (1) $\mu''(f, H_{bias})$ for typical parameters of magnetron-sputtered iron films: $M_S = 21.5$ kOe, $H_A = 70$ Oe, $\alpha = 0.05$; (b) The $\mu''(f, H_{bias})$ surface of the same film with the account of eddy currents (5) for $d = 2 \times 10^{-6}$ m and $\sigma = 1.03 \times 10^7$ Ohm×m.

of complex permeability $\mu''(f, H_{bias})$ for typical FMR parameters observed for magnetron-sputtered iron films.

It is easy to see that SF-VNA and SB-FMR measurements are presented by corresponding cross-sections of this surface. In case of fixed-bias measurements of a thin film, rel. (1) is readily transformed into a Lorenz line

$$\mu\left(f, H_{bias}\right) = 1 + \frac{\mu_0\left(H_{bias}\right) - 1}{1 - \dfrac{f^2}{F^2} + i\Gamma\dfrac{f}{F}} \tag{2}$$

where $\mu_0(H_{bias})$ is the static permeability, F is the resonance frequency, Γ is the damping factor. The Lorenz parameters are readily expressed in terms of LLG rel. (1):

$$F = \gamma\mu_{vac}\sqrt{M_S\left(H_A + H_{bias}\right)} \tag{3a}$$

$$\mu_0\left(H_{bias}\right) = \frac{M_S}{H_A + H_{bias}} + 1 \tag{3b}$$

$$\Gamma = \alpha\sqrt{\frac{M_S}{H_A + H_{bias}}} \tag{3c}$$

The latter relation (3c) shows that the FMR linewidth decreases with bias increase. Further we shall apply to magnetic absorption in terms of Gilbert's damping factor α, as contrary to Lorenz's damping factor Γ the former is an intrinsic property of a substance and does not depend on external bias.

Theoretically SF-VNA and SB-FMR techniques are equivalent, the difference is in the source of measurement errors. The reflectivity $R(f)$ data are affected by calibration errors that arise from inaccuracy of determination of S-parameters of coaxial to strip junction as well as from radiation from the cell and multipole resonance of conductive samples. These very errors limit the operating frequency band of SF-VNA technique and make the experimental $\mu(f)$ curves much less smooth than the $\mu(H_{bias})$ curves, as these errors are mostly bias independent. The resultant SNR of SB-FMR data is approximately 50 times lower than that of SF-VNA data obtained with the same experimental setup (Fig. 1).

The main drawback of conventional SB-FMR technique is that the measured reflectivity response $\Delta R(H_{bias})$ is uncalibrated in magnitude; therefore $\Delta R(H_{bias})$ can not be directly related to $\Delta\mu''(H_{bias})$ and the parameters (M_S, H_A and α) of a permeable sample are usually determined from the bias dependence of a resonance frequency (rel. (3a)). In case of a calibrated cell it seems promising to determine

these parameters from a single $R(H_{bias})$ measurement. The simulation shows that for a thin permeable film M_S, H_A and α can be found by numerical fit of rel. (1) with synthetic data displayed in Fig. 2. The FMR parameters are readily fitted for an arbitrary $f = const$ cross-section. The uncertainty grows where the film thickness d is close to or exceeds the microwave penetration depth (skin-depth) δ, in this case we must take into account the contribution of eddy currents.

4. EFFECT OF EDDY CURRENTS

For metals the microwave permittivity ε is a function of electrical conductivity σ and frequency f: The penetration depth δ of permeable metals contrary to that of impermeable ones is not a monotonous function of frequency and depends on external bias [13]:

$$\delta = \frac{c}{2\pi f \mathrm{Im}\sqrt{\varepsilon\mu}} \approx \frac{1}{\mathrm{Re}\sqrt{\pi f \sigma \mu \mu_{vac}}} \tag{4}$$

where $c = 3 \times 10^{10}$ m/sec, $\mu_{vac} = 1.257 \times 10^{-6}$ Hn/m, $\sigma = 1.03 \times 10^7$ Ohm×m for iron.

The $\delta(f)$ graph in Fig. 3 is calculated based on the permeability and conductivity of the infinite iron film with $\mu''(f, H_{bias})$ displayed in Fig. 2. If the film permeability is frequency independent (the case of an impermeable alloy), the penetration depth decreases with frequency as

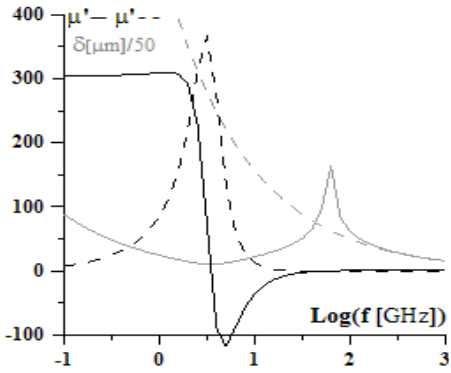

Figure 3. The reconstructed frequency dependence of permeability (solid and dashed black lines) and skin-depth. The solid grey line presents skin-depth for Fe-based film with FMR spectrum displayed in Fig. 2(a), the dashed grey line presents skin-depth for the same film with $\mu = 1$.

$\delta(f) \sim 1/\sqrt{f}$. In case of a permeable metal the function $\delta(f)$ is more complicated and depends on the shape of FMR spectrum. In case of the Lorenzian line of absorption it is easy to derive that there are two extremums of $\delta(f)$ function.

Namely, the skin-depth δ is minimal $\delta_{\min} = 1/\sqrt{2\pi F\sigma\mu_{vac}(\mu_0 - 1)}$ at the resonance frequency F, and δ is maximal $\delta_{\max} = 1/\sqrt{\sigma\mu_{vac}\pi f(|\mu| + \mu'')}$ at the frequency where $(|\mu| + \mu'')$ is minimal. As $\mu(f)$ is most steep in the vicinity of FMR, the penetration depth there is almost frequency independent contrary to that of impermeable materials (compare grey curves in Fig. 3). It is easy to show that the external bias does not affect the minimal penetration depth as the increase of FMR frequency F is compensated with the permeability decrease $\delta_{\min} = \sqrt{\alpha}/\mu_{vac}\sqrt{\gamma\sigma M} \approx 2.26\,\mu\text{m}$. For the properties of the film displayed in Fig. 2 $\delta_{\min} \approx 0.226\,\mu\text{m}$.

Now we come to the effect of film thickness on the parameters of FMR absorption line. In reality it is impossible to exclude the gaps between the sample and the cell base (see Fig. 1), therefore the film is irradiated from both surfaces (mind that δ is a single side penetration depth) and the measured permeability μ_{meas} is related to film intrinsic permeability [5, 11] μ_{film} as

$$\mu_{meas} = \mu_{film}\frac{\tan\theta}{\theta} \text{ where } \theta \approx i\frac{d}{2\delta} \approx \frac{d}{2}\sqrt{-i2\pi f\mu_{vac}\mu_{film}\sigma} \qquad (5)$$

Numerical calculations show that eddy currents distort the shape of $\mu''(f)$ dispersion in case of a thick film, but do not affect the shape of $\mu''(H_{bias})$ curves (Fig. 2(b)). The bias dependence of resonant frequency $F(H_{bias})$ is the same parabola described by rel. (3a), the only difference is that the magnetic response (the peak value of μ'') is significantly decreased (compare Fig. 2(a) and Fig. 2(b)). This decrease of magnetic response is the reason of rough errors in M_S and H_A determined in a single frequency SB-FMR measurement. The errors reveal themselves as the false dependence of M_S and H_A on measurement frequency f. The lower is the response amplitude $\mu_0 - 1 = \left(\frac{M_s}{f/\gamma\mu_{vac}}\right)^2$ obtained from fixed-frequency measurements, see Eq. (1), compared to the value $\mu_0 - 1 = \frac{M_S}{H_A}$ calculated from $F(H_{bias})$ function (rels. (3a), (3b)), the stronger is the false $M_S(f)$ and $H_A(f)$ dependence obtained by direct fitting of M_S and H_A at fixed frequencies and the higher is the d/δ ratio. Note that to determine M_S and H_A parameters from Eqs. (3a) and (3b) one needs to perform at least 4–5 SB-FMR measurements at different frequencies.

The quantitative estimation of d/δ ratio is possible if the absorption line is still of the Lorenzian shape. In case for $0 < |\theta| \approx \frac{d}{2\delta} < \pi$ the skin-dependent factor in Eq. (5) is simplified as

$$\frac{\tan\theta}{\theta} \approx \frac{1}{1-\theta^2/3} \approx \frac{12}{12+2\pi i d^2 \sigma f \mu_{vac}\mu_{film}} \tag{6}$$

Taking into account Eq. (5) and introducing the factor $\frac{\tan\theta}{\theta}$ into the Lorenz formula (2) it is easy to see that the damping factor Γ in Eq. (2) is increased by eddy currents as

$$\Gamma(d) = \Gamma(0) \times \left[1 + \frac{1}{12}\left(\frac{d}{\delta}\right)^2\right] = \alpha\sqrt{\frac{M_S}{H_A + H_{bias}}} \times \left[1 + \frac{1}{12}\left(\frac{d}{\delta}\right)^2\right] \tag{7}$$

where $\Gamma(0)$ is the damping factor of an infinitely thin film ($d = 0$).

The zero-frequency response for zero thickness is $\mu_0(H_{bias}, 0) - 1 = \mu''_{peak}\Gamma = \frac{M(0)}{H_A(0)+H_{bias}}$, for thickness d the response is the same $\mu_0(H_{bias}, d) - 1 = \mu''_{peak}(d)\,\Gamma(d) = \frac{M_S(d)}{H_A(d)+H_{bias}}\left[1 + \frac{1}{12}\left(\frac{d}{\delta}\right)^2\right]$, therefore comparing the calculated for thickness d response and the one for zero thickness, Eq. (3a), it is possible to estimate the penetration depth δ. As a result we get the relative thickness of metal:

$$\frac{d}{\delta} = 3.46\sqrt{\left(\frac{M_S(0)}{M_S(d)}\right)^2 - 1} = 3.46\sqrt{\frac{M_S(0)}{H_A(0)+H_{bias}}\frac{H_A(d)+H_{bias}}{M_S(d)} - 1} \tag{8}$$

Simulations of measurement of thin and thick films with permeability displayed in Fig. 2 are shown in Fig. 4.

Note that for thick metal films $\mu(f)$ curves differ from Lorenzian ones in shape, while $\mu(H_{bias})$ curves are only shifted from Lorenzian ones by a frequency-dependent complex constant (see Fig. 2). This constant corresponds to bias-independent diamagnetic effect of eddy currents and their contribution to magnetic losses. Therefore to describe the experimental data it is necessary to include for fitting an additional free parameter (a complex value). In real measurements this free parameter includes the other bias-independent contributions (the radiation losses, the inaccuracy of permittivity account, etc.) as well.

The false dependence of the penetration depth on bias (Fig. 4(a)) is a result of the distortion of Lorenz lineshape for thick metal under low bias (Fig. 2). The fitting accuracy decreases with the decrease of H_{bias} and correspondingly with the shift of the measurement frequency to that of the zero-bias FMR. The slope ratio of $F^2(H_{bias})$-line (black

circles in Fig. 4(b)) is mainly defined by high-bias data and therefore presents more accurate estimation. The penetration depth exceeding the calculated $\delta = 0.226\,\mu\text{m}$ for $d < 1\mu\text{m}$ (Fig. 4(b)) reveals the exponential nature of the skin-layer.

The above account for eddy currents has a serious limitation: the film under study is assumed to have a simple spectrum with a single FMR line. Emulation reveals that the distribution of damping factors α over a set of values causes the decrease of magnetic response and the distortion of permeability spectrum $\mu(f)$ similar to that by eddy currents. The admixture of several magnetic phases with different M_S and H_A values is simpler to detect than a set of α-values as it causes the split of the absorption line increasing with bias increase. Both effects make the fitting procedure inaccurate and mask the contribution of eddy currents; in the case of heterogeneous film the measured response may exceed the response calculated from the $F^2(H_{bias})$ curve, rel. (3a).

5. EXPERIMENTAL RESULTS

The described technique is applied to determine M_S, H_A and α of Fe-based magnetron-sputtered films [15]. To suppress the eddy currents

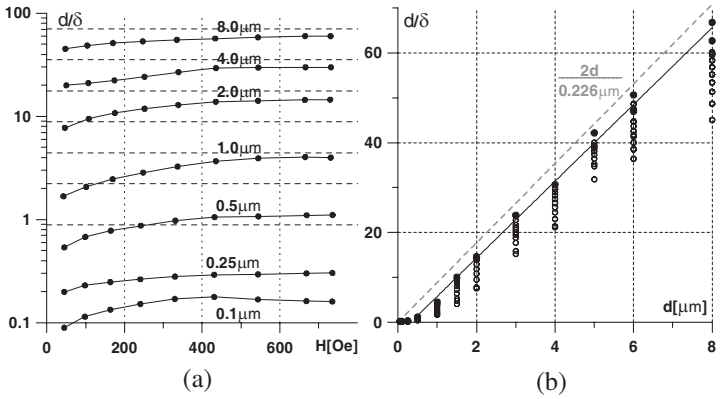

Figure 4. Measurement simulation of the metal film with permeability dispersion displayed in Fig. 2 ($M_S = 21.5\,\text{kOe}$, $H_A = 70\,\text{Oe}$, $\alpha = 0.05$, $\sigma = 1.03 \times 10^7\,\text{Ohm}\times\text{m}$). The dashed grey line corresponds to the penetration depth $\delta = 0.226\,\mu\text{m}$ calculated from the peak permeability and electrical conductivity data (rel. (4)). The empty circles correspond to bias-dependent data displayed in the left graph. The filled circles correspond to data calculated from rel. (3a) for $M(0)$ and $H_A(0)$ and for $M(d)$ and $H_A(0)$.

the metal films are separated by 0.07 μm-thick SiO_2 interlayers. The total thickness of metal on a substrate varies from 0.35 to $\sim 2\,\mu$m. The zero-bias absorption spectra of the measured films are displayed in Fig. 5. The thin ($5 \times 0.07\,\mu$m) film on glassceramics displays a Lorenzian absorption line with a low damping factor. The thicker film ($30 \times 0.07\,\mu$m) shows a distortion like that by eddy currents (see. Fig. 2(b)), while the film on a Mylar substrate displays an intermediate broad line of absorption. The 1 hour 300°C anneal of samples with glassceramic substrates totally destroys the microwave absorption. The difference in these spectra seems difficult to explain, but the multifrequency SB-FMR measurements partially clear the situation.

The results of these measurements are brought together in Table 1. For comparison the first two rows display the simulation results for a 0.1- and 2.0 μm-thick Fe film. The negative value of anisotropy field fitted for annealed samples is a formal parameter indicating that the magnetisation is parallel to $\vec{H}$-vector and there is no zero-bias resonance [3, 11].

The main drawback of the proposed technique is that the data treatment is based on an assumed structure of sample under study.

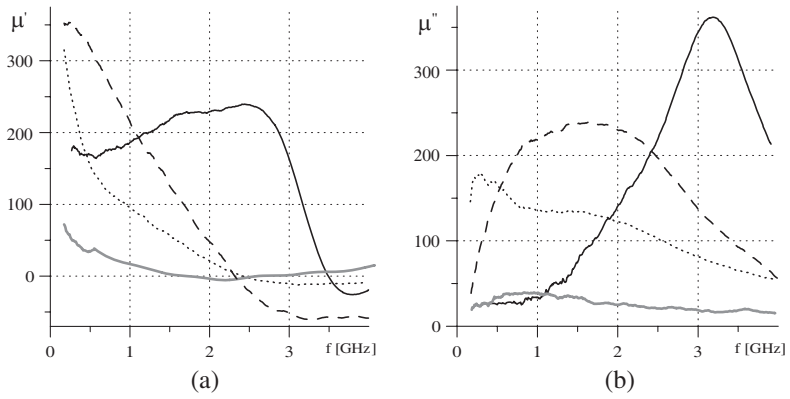

Figure 5. Permeability spectra of Fe-based films sputtered on 12 μm-thick Mylar and 500 μm-thick glassceramic substrates. Dashed black line corresponds to $15 \times 0.07\,\mu$m-thick Fe layers on Mylar substrate, solid black line corresponds to $5 \times 0.07\,\mu$m-thick Fe layers on glassceramics, dotted black line corresponds to $30 \times 0.07\,\mu$m-thick Fe layers on 500μm-thick glassceramics, thick grey line corresponds to the same $30 \times 0.07\mu$m-thick Fe layers on glassceramics after 1-hour anneal at 300°C (practically overlaps with the annealed $5 \times 0.07\,\mu$m-thick sample).

Table 1.

Initial data		fitted data					calculated data	
substrate & treatment	d [μm]	M_S [kOe]	H_A [Oe]	$\alpha_{\min}$	$\alpha_{\max}$	$2d/\delta$	F_0 [GHz]	μ_0
synthetic data	0.1	21.5	70	0.051	0.051	0.168	3.43	307
synthetic data	2.0	21.5	70	0.081	0.112	14.6	3.43	307
mylar	15×0.07	19.9	13.7	0.034	0.043	36.6	1.46	1452
glassceramics	5×0.07	19.89	65.62	0.026	0.030	8.78	3.20	303
annealed at 300°C for 1 hr	5×0.07	20.58	−25.91	0.026	0.044	22.69		
glassceramics	30×0.07	17.2	30.6	0.071	0.109	18.17	2.01	572
annealed at 300°C for 1 hr	30×0.07	19.6	−33.3	0.045	0.129	31.95		

The drawback from the engineering viewpoint is that the obtained data may differ from that of zero bias SF-VNA measurements, where the contribution of a non-uniform magnetisation is essential.

It is easy to see (Table 1 and Fig. 5) that there is a qualitative agreement between the calculated zero-bias static permeability μ_0 and resonance frequency F_0 only in case of a simple FMR spectrum (glassceramic substrates). An indirect sign that the measured FMR spectrum is a simple Lorenzian line is the damping factor stability, the variation of α with bias indicates that FMR spectra are complicated. In this case F_0 and μ_0 are far from the parameters measured by the SF-VNA technique. Nevertheless the increase of physical thickness of metal layer is correlated to the increase of the relative thickness $2d/\delta$, therefore the insulation with SiO_2 interlayers seems ineffective. The anisotropy field of iron films arises from the mechanical strain similar to [14]: the magnetron-sputtered metal is tempered, the more rigid is the substrate, the higher is the mechanical strain and the higher are H_A and F_0, correspondingly. An anneal removes the temper thus destroying the anisotropy field and zero-bias resonance as well. The film on a Mylar has a low anisotropy field as a flexible substrate readily removes the strain from metal.

6. CONCLUSION

The proposed multifrequency SB-FMR technique has several advantages over the standard SF-VNA measurements. First of all as the mea-

surements are performed at fixed frequencies, the frequency-dependent errors are subtracted and the signal to noise ratio (SNR) significantly ($\sim$50 times) exceeds that of the field domain technique.

The SB-FMR measurements performed at a set of frequencies exceeding the FMR frequency make it possible to determine both the composition-dependent (M_S) and the structure-dependent (H_A, α) properties of a permeable film without the data on the amount of permeable substance. Particularly the measurements relate the effects of substrate flexibility and annealing with the anisotropy field H_A of a sputtered film.

The developed technique makes it possible to estimate the ratio of penetration depth to sample thickness studying a single multilayered film. The drawback is that in case of a multiline FMR spectrum the account for contribution of eddy currents is much more complicated and the above procedure may lead to rough errors in penetration depth. Besides the data treatment procedure of multifrequency SB-FMR technique is cumbersome, as fitting algorithms are developed for smooth functions, while the distorted by errors experimental data exhibit multitude of local minima.

ACKNOWLEDGMENT

The research is partially supported by the RFBR grants No. 09-08-01161 and No. 07-08-92111.

The authors wish to thank S. A. Maklakov and I. A. Ryzhikov for sputtering of the test samples.

REFERENCES

1. Bozorth, R. M., *Ferromagnetism*, IEEE Press, New York, 1993.
2. Neudecker, I., G. Woltersdorf, B. Heinrich, T. Okuno, G. Gubbiotti, and C. H. Back, "Comparison of frequency, field and time domain ferromagnetic resonance methods," *Journal of Magnetism and Magnetic Materials*, Vol. 307, 148, 2006.
3. Kalarickal, S. S., P. Krivosic, M. Wu, C. E. Patton, M. L. Shnider, P. Kabos, T. J. Silva, and J. P. Nibarger, "Ferromagnetic resonance linewidth in metallic thin films: Comparison of measurement methods," *Journal of Applied Physics*, Vol. 99, 093909, 2006.
4. Starostenko, S. N., K. N. Rozanov, and A. V. Osipov, "A broadband method to measure magnetic spectra of thin films," *Journal of Applied Physics*, Vol. 103, 07E914, 2008.

5. Getman, A., A. Sivov, N. S. Perov, I. T. Iakubov, K. N. Rozanov, I. A. Ryzhikov, and S. N. Starostenko, "Static and dynamic magnetic properties of Fe films," *Journal of Magnetism and Magnetic Materials*, Vol. 272–276, e909, 2004.
6. Iakubov, I. T., A. N. Lagarkov, S. A. Maklakov, A. V. Osipov, D. A. Petrov, K. N. Rozanov, and I. A. Ryzhikov, "Laminates of multi-layered Fe films for microwave applications," *Journal of Magnetism and Magnetic Materials*, Vol. 316, e813, 2007.
7. Starostenko, S. N. and K. N. Rozanov, "Resonantly enhanced strip-line technique to measure microwave permeability of thin films," *Journal of Magnetism and Magnetic Materials*, 2009.
8. Mason, S. J., "Feedback theory-some properties of signal flow graphs," *Proc. IRE*, Vol. 41, 1144–1156, 1953.
9. Rozanov, K. N., N. A. Simonov, and A. V. Osipov, "Microwave measurements of the magnetic film permeability," *J. Comm. Technology and Electronics*, Vol. 47, No. 2, 210–216, 2002.
10. Adenot, A. L., O. Acher, D. Pain, F. Duverger, M.-J. Malliavin, D. Damiani, and T. Taffary, "Broadband permeability measurement of ferromagnetic thin films or microwires by a coaxial line perturbation method," *Journal of Applied Physics*, Vol. 98, No. 9, 5965–5967, 2000.
11. Lagarkov, A. N., K. N. Rozanov, N. A. Simonov, and S. N. Starostenko, "Microwave permeability of thin films," *Handbook of Advanced Magnetic Materials*, Vol. 4, Springer, 2005.
12. Lofland, S. E., H. Garcia-Miquel, M. Vazquez, and S. M. Bhagat, "Microwave magnetoabsorption in glass-coated amorphous microwires with radii close to skin depth," *Journal of Applied Physics*, Vol. 92, No. 4, 2058–2063, 2002.
13. Starostenko, S. N., K. N. Rozanov, and A. V. Osipov, "Microwave properties of composites with glass coated amorphous magnetic microwires," *Journal of Magnetism and Magnetic Materials*, Vol. 298, 56–64, 2006.
14. Acher, O., J. L. Vermeulen, A. Lucas, P. Baclet, J. Kazanjoglou, and J. C. Peuzin, "Direct measurement of permeability up to 3 GHz of co-based alloys under tensile stress," *Journal of Applied Physics*, Vol. 73, No. 10, 6162–6164, 1993.
15. Iakubov, I. T., A. N. Lagarkov, S. A. Maklakov, A. V. Osipov, K. N. Rozanov, I. A. Ryzhikov, V. V. Samsonova, and A. O. Sboychakov, "Microwave and static magnetic properties of multi-layered iron-based films," *Journal of Magnetism and Magnetic Materials*, Vol. 321, 726–729, 2009.